

THREE DIMENSIONAL DYNAMIC STRESS ANALYSIS AROUND A MOVING CRACK AND SIMULATION OF AE

K. Katsuyama and Y. Sato

*Mining and Safety Division, National Research Institute for Pollution and Resources,
16-3 Onogawa, Yatabe, Tsukuba, Ibaraki, Japan*

ABSTRACT

A numerical analysis of the three dimensional dynamic stress distribution around a crack tip which moves in a prismatic brittle bar with a notch under the static tensile loading is presented. The numerical procedure is based on the finite difference method. It is analysed that the dynamic stress distributions are different from those of the static problems because of rarefaction waves from the moving crack, curvature of the crack front and the reflected waves from the surface of the prism. Simulation of AE caused by the moving crack is also presented, and it is mentioned that the moving crack has great influence on the AE wave form.

KEYWORDS

Three dimensional stress analysis, Dynamic stress, Acoustic emission, AE, Numerical stress analysis, Moving crack, Dynamic crack

INTRODUCTION

The three dimensional dynamic stress distribution in a rock with one free face caused by propagation of a wave by an explosion was solved analytically by Ito and Sassa(1963a). With advancement of a huge computer, the numerical analysis of the dynamic stress distribution caused by a propagation of a wave has been tried. Ito and Sassa approached the problem of the dynamic stress distribution in an infinite elastic material which included the breakage phenomena with a numerical method of finite difference approximation(1972a). Katsuyama and others approached the dynamic stress concentration around a cylindrical hole by the numerical method(1972b), and also approached the dynamic stress distribution caused by a smooth blasting which had a hole in a solid with one free face, and simulated the growth of cracks in the case of a smooth blasting(1973). Niwa and others approached the similar problem with the method of finite difference method and FEM(1974). Most of the three dimensional problems by FEM were static, and most of these dynamic stress analysis were two dimensional problems. Three dimensional dynamic stress analysis needs so huge capacity of a computer that Boundary Element Method is tried to use for analysis of the dynamic stress distribution around a structure buried in the ground (Niwa and others,1976).

Most of three dimensional problems about the stresses near the tip of a flaw or a notch could be replaced with their two dimensional problems which were discussed by Sneddon(1940), Irwin(1957b) and so on. When the acoustic emission (AE) caused by a fracture of the material is discussed, attenuation of amplitude of AE wave from the source cannot be neglected. Though it is said that the primitive wave form and the frequency spectrum of AE wave has a lot of information about a mechanism of fracture and deformation, it is very hard to measure the primitive wave of AE and to get the spectrum of it as the wave measured includes a lot of reflected wave. And it is presumed that the velocity of crack propagation has effect on the AE wave form in the case that the velocity is high. So, it is very important for detecting AE and studying the breakage status to analyse the three dimensional dynamic stress distribution near the crack tip.

In this paper, therefore, the investigation of the fracture of a prismatical bar with a notch under tensile static loading is undertaken and growth of a dynamic crack from the notch is simulated. And the three dimensional stress distribution in the prism is also analysed and AE wave form which appear on the surface of the prism are discussed.

METHOD OF THREE DIMENSIONAL DYNAMIC STRESS ANALYSIS

The method of three dimensional dynamic stress analysis caused by a propagation of elastic wave adopted in this paper is the finite different approximation approached by Maechen and Sack(1963b). The acceleration of a nodal point (a point of Lagrangian coordinates) at $t=t_0$ is calculated with the method of the finite different approximation using the equation of motion expressed with Lagrangian coordinates which is applied in the stress field at $t=t_0$. The displacement of the nodal point at $t=t_0$ is obtained by integrating the acceleration twice with respect to time. And the strain in a cubic element enclosed with eight nodal points is calculated using these displacements. And then the new stress field at $t=t_0+\Delta t$ is calculated applying the elastic constants to this strain. Like this, the dynamic stress distribution and vibration at each nodal point is numerically obtained.

MODEL FOR NUMERICAL ANALYSIS

The model for simulation of process of the crack growth from the notch under the three dimensional dynamic stress distribution is as shown in Fig. 1. This prismatical bar which is 20cm in length, 3cm in width and 3cm in thickness has a notch of 5mm in depth. The magnitude of the applied uniform tensile loading is increased from 0 to p so slowly that the natural frequency of the model is negligible. Uniform loading is constant after the crack from the notch tip begins to move. The model is divided into many cubic elements of 1mm in side length as shown in Fig. 2. The part calculated is a quarter of the model which is drawn in bold lines taking advantage of symmetry of the problem.

TABLE 1 Mechanical Properties

Velocity of longitudinal wave	$C_L = 5000\text{m/s}$
Velocity of transverse wave	$C_T = 3140\text{m/s}$
Velocity of Rayleigh wave	$C_R = 2846\text{m/s}$
density	$\rho = 2.7\text{ gr/cm}^3$
poison's ratio	$\nu = 0.174$
tensile strength	$S_t = 40\text{ kg/cm}^2$

Cubic element's number is 45000 and Δt is $0.15\mu\text{s}$. The CPU time is about 11hrs 30 mins to calculate 2180 times over until $t=327\mu\text{s}$. The computer used is FACOM M200 in the RIPS computer centre. Marble is considered as the brittle material of the model, and the mechanical properties of it are given in Table 1. Brittle fracture begins when the maximum principal stress of the element becomes the tensile strength, and the nodal points on the surface L_0 as shown in Fig. 1 can move freely in the y -direction.

COMPARISON WITH THEORETICAL RESULTS

In the case that the tensile loading increases very slowly that the wave motion doesn't occur in the model and the natural frequency of the model is negligible, the stress distribution obtained by our method is respected to be the same as the result of the static problem. Fig. 3 (a) and (b) show the results of calculation for model as shown in Fig. 3 (c). The contour line of normal stress σ_y around the notch is shown in Fig. 3 (a) and the stress distribution of σ_y along x -axis is shown in Fig. 3 (b). Let the crack tip be the origin of polar coordinates (r, θ) and let K_I be the stress concentration factor of mode I, then σ_y near the notch is given by Eq. (1) (William, 1957a), (Irwin, 1957b).

$$\sigma_y = \frac{K_I}{\sqrt{2\pi r}} \left\{ \cos \frac{\theta}{2} \left(1 + \sin \frac{\theta}{2} \sin \frac{3\theta}{2} \right) \right\} \quad (1)$$

The line shows the theoretical result obtained by Eq. (1), \bullet shows the result of the numerical analysis obtained by us. In Fig. 3 (a) and (b), our result by numerical analysis agrees fairly well with theoretical result.

RESULTS

Dynamic Stress Distribution

Three dimensional dynamic stress distributions are as shown in Fig. 4. The value of the contour is 15 kg/cm^2 of tensile stress σ_y . The stress distribution at $N=1924$ is the same as static stress distribution. The stress on the surface at $z=1.5\text{cm}$ is smaller than that in the interior. At $N=1927$, the part concentrated by the stress moves to the right in order that the crack tip moves to the right, and the rarefaction waves are projected into the prism from the crack surface (Katsuyama and others, 1970). So, the stresses of zone "a" become smaller. The stresses of zone "b" and "c" have no change yet, but they are almost the same as the stresses at $N=1924$. At $N=1931$, it is clear that the stress of zone "d" decrease very much because of the rarefaction wave from the crack surface though the stress of zone "e" is still the same as it at $N=1924$. At $N=1935$, the zone of "f" is under the larger influence of the rarefaction wave, and the stress distribution of the zone "g" is fairly different from it of $N=1924$. But the stress distribution of zone "h" does not change so much. This reason is explained by the model of tensile dislocation which is shown in Fig. 5(a). The distribution of the amplitude of longitudinal waves projected from the tensile dislocation face is as shown in Fig. 5(b) (Otsu, 1983). The amplitude of longitudinal waves of y -direction is about 5 times bigger than that of x -direction.

It is said generally from Fig. 4 comparing with the static stress distribution of σ_y that a part of the contour of $y = 15\text{kg/cm}^2$ denoted by "i" is high, a part of the contour denoted by "j" is low and a part of the contour on the surface of the prism is high. This trend of the distribution is explained with the reason that the waves projected from the crack tip reflect at the

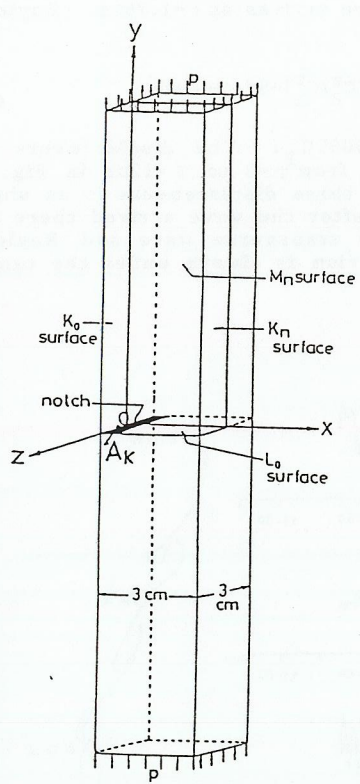


Fig. 1 Model for numerical analysis of which dimensions are 20cmx 3cmx3cm and the Euler coordinates (x,y,z)

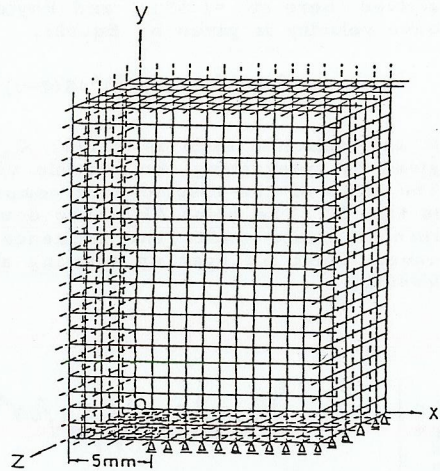


Fig. 2 Divided cubic elements near the notch of which depth is 5mm

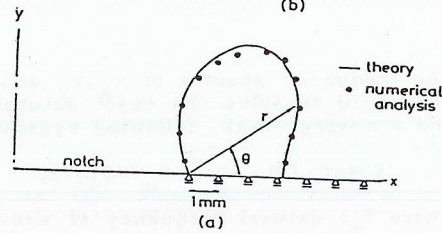
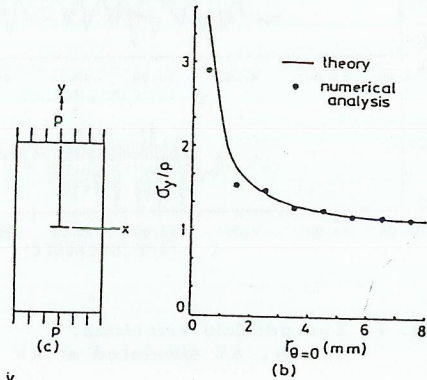


Fig. 3 Numerical stress distributions around the notch under the tensile loading which is increasing very slowly and the theoretical static stress distribution

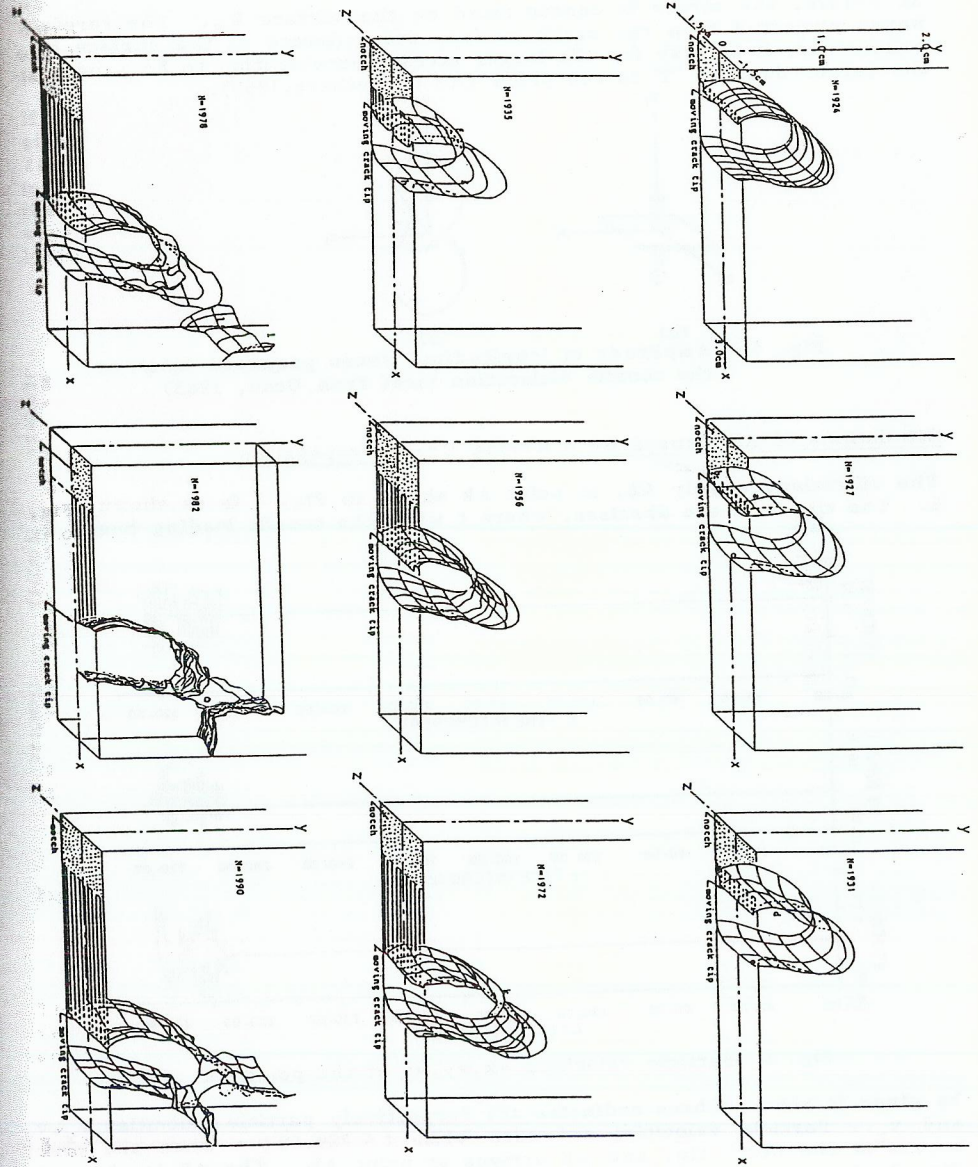


Fig. 4 Three dimensional dynamic stress distributions around a moving crack (N=1924: t=288.60μs)

surface of $z=\pm 1.5\text{cm}$ and the stress is concentrated in order that the crack grows more slowly at $z=\pm 1.5\text{cm}$ than the other part.

At $N=1978$, the stress is concentrated on the surface K_N . The rarefaction waves projected from the crack surface are reflected at the surface of the prism. So, it is easy for the larger stress concentration to be produced at the corner denoted "1" in the prism (Ito and others, 1969).

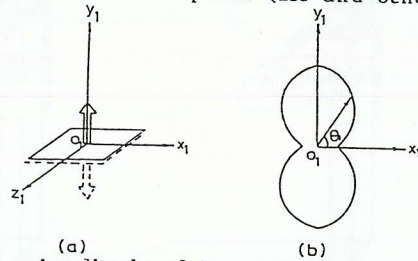


Fig. 5 Amplitude of longitudinal waves projected from the tensile dislocation face (from Otsu, 1983)

Simulations of AE Caused by a Moving Crack Propagation

The vibration, namely AE, of point Ak shown in Fig. 1 is as shown in Fig. 6. The time t is the abscissa, where t when the tensile loading began to

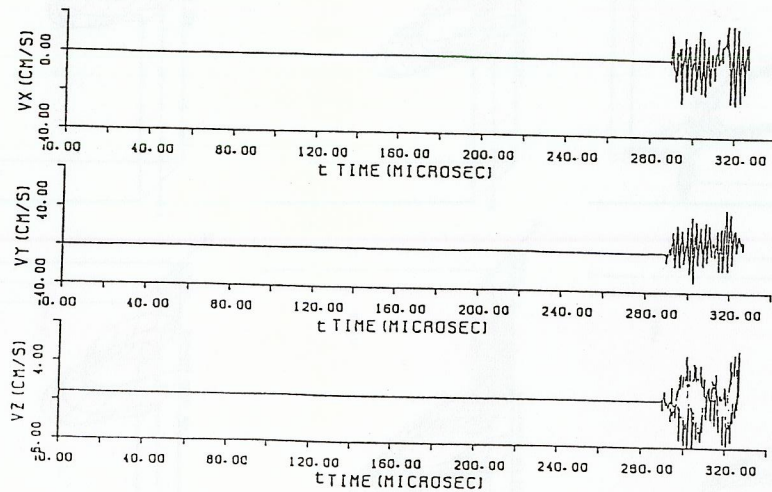


Fig. 6 Particle velocities v_x, v_y, v_z at the point Ak

be given is zero. Three ordinates are respectively particle velocities v_x, v_y and v_z . Particle velocities are zero while $t < 289.60 \mu\text{s}$ when the crack occurs at the notch tip, and AE arrives at point Ak. The AE is shown in Fig. 7 of which abscissa is the time τ . τ is zero when the crack was created at the notch tip. The ordinates is the same with that of Fig. 6.

It takes $1 \mu\text{s}$ denoted by "p" in Fig. 8 that the longitudinal wave from the crack tip arrived at point Ak. It is reasonable that the point Ak moves in

the (-x)-direction at first as shown in Fig. 5. The transverse wave arrived there at $\tau=1.59 \mu\text{s}$, and Rayleigh wave arrives at $\tau=1.76 \mu\text{s}$. Rayleigh wave velocity is given by Eq.(2).

$$(C_R^2/C_T^2)^3 - 8(C_R^2/C_T^2)^2 + 8(2-\nu)/(1-\nu) \times (C_R^2/C_T^2) - 8/(1-\nu) = 0 \quad (2)$$

If the poisson's ratio is 0.174, C_R is $0.9065 C_T$. The displacements are given by integrating the particle velocities from $\tau=0$ to $\tau=12 \mu\text{s}$ in Fig. 7. The locus of the displacement composed of three displacements is as shown in Fig. 8. The point Ak moves down just after the wave arrived there and then it rotate under the influence of the transverse wave and Rayleigh wave. Point Ak goes up rotating as the prism is always under the tensile loading.

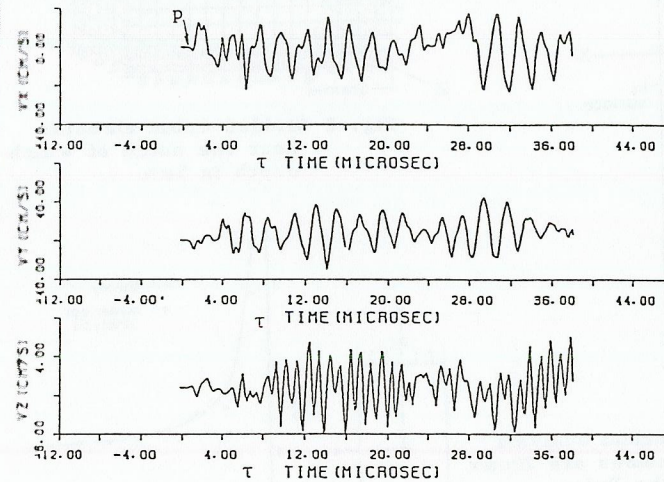


Fig. 7 The particle velocities, namely, AE simulated at Ak

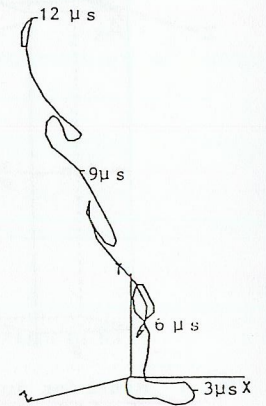


Fig. 8 The locus of the displacement at the point Ak

The frequency spectra of v_x, v_y and v_z are as shown in Fig. 9. As it is very hard to solve the exact natural frequency of the prism with a notch and a moving crack, following equations are used for discussion.

$$f_n = n C_L / 2l, \quad f_n = n C_T / 2l, \quad n=1,2,3,\dots \quad (3)$$

where f : natural frequency of mode n , l : length of a bar with two free ends. And following equation are also used.

$$f_k = (2k-1) C_T / 4l, \quad f_k = (2k-1) C_R / 4l, \quad k=1,2,3,\dots \quad (4)$$

where f_k : natural frequency of a bar with one free end and one fixed end. Peak "a" denoted in F_vx and F_vz is the natural frequency of mode 1 for

the width and the thickness of the prism caused by the transverse wave and peak "b" is it caused by the longitudinal wave. Peak "c" shown in

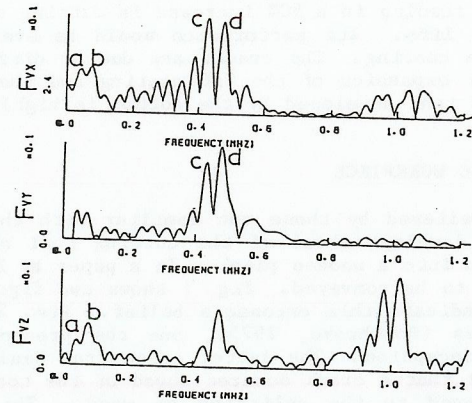


Fig. 9 Fourier analysis of the AE waves simulated at Ak shown in Fig. 7

Fvx and Fvy is the natural frequency of mode 2 obtained by solving Eq.(4) for the 5mm depth of the notch caused by Rayleigh wave and peak "d" is also natural frequency of mode 2 caused by transverse wave. We can see a lot of influence of original length of notch on the AE wave as shown in Fig. 9.

REFERENCES

- Ito, I. and Sassa, K. (1963a) : J. Mining and Metallurgical Institute of Japan, 86, 984, p.195
- Sassa, K. and Ito, I. (1972a) : J. Society of Material Science, 21, 221, p.123
- Katsuyama, K., Sassa, K. and Ito, I. (1972b) : J. Society of Material Science, 21, 228, p.839
- Katsuyama, K., Sassa, K. and Ito, I. (1973) : J. Mining & Metal. Inst. of Japan, 89, 1019, p.7
- Niwa, Y., Kobayashi, S. and Matsumoto, T. (1974) : J. Society of Material Science, 23, 248, p.43
- Niwa, Y., Kobayashi, S., Fukui, T. and Azuma, N. (1976) : Pro. Japan Soc. Civil Eng., no.248, p.41
- Sneddon, I.N. (1940) : Pro. Roy. Soc. Lond. (A) 187, p.229
- Irwin, G.R. (1957b) : J. Appl. Mech., 24, 361
- Maechen, G. and Sack, S. (1963b) : Methods in Computational Physics, vol.3, Academic Press Willian, M.L. (1957a) : J. Appl. Mech., 24, 109
- Irwin, G.R. (1957b) : J. Appl. Mech., 24, 361
- Katsuyama, K., Sassa, K. and Ito, I. (1970) : J. Mining & Metal. Inst. of Japan, 86, 984, p.195
- Otsu, M. (1983) : J. Society of Material Science, 32, 356, p.579
- Ito, I., Sassa, K. and Shigematsu, K. (1969) : J. Mining & Metal. Inst. of Japan, 85, 969, p.1